Nuclear Science
2021; 6(3): 18-25
http://www.sciencepublishinggroup.com/j/ns
doi: 10.11648/j.ns.20210603.11
ISSN: 2640-4338 (Print); ISSN: 2640-4346 (Online)

Investigation of Alignment Effects of Neutron and Proton Pairs in High Spin States of Band Crossing for ^{159,160}Sm Isotopes Using Projected Shell Model (PSM)

Mohammad Reza Pahlavani*, Malihe Teimoori

Department of Physics, University of Mazandaran, Babolsar, Iran

Email address:
m.pahlavani@umz.ac.ir (M. R. Pahlavani)

*Corresponding author

To cite this article:
Mohammad Reza Pahlavani, Malihe Teimoori. Investigation of Alignment Effects of Neutron and Proton Pairs in High Spin States of Band Crossing for ^{159,160}Sm Isotopes Using Projected Shell Model (PSM). *Nuclear Science.* Vol. 6, No. 3, 2021, pp. 18-25.
doi: 10.11648/j.ns.20210603.11

Received: September 14, 2021; **Accepted**: October 11, 2021; **Published**: October 28, 2021

Abstract: Energy spectrum of nucleus is one the important information for better recognition of nuclear force and interaction of nucleon inside of the nucleus. Energy levels of nucleus are measured by detecting gamma- ray energy spectrum when a target nucleus bombarded with a special projectile to excite it in to levels higher than ground state. On the other hand, there are several models to calculate nuclear energy levels. Solution of the Schrödinger equation by considering a suitable potential is direct method to obtain energy levels of a quantum mechanical system like nucleus. Projected shell model is a model of this type that is developed by solving the Schrödinger equation for a set of potentials along with role of spin. Band structure and yrast bands for even-even and odd-even isotopes of Samarium (^{159,160}Sm) are calculated using a Fortran code founded based on the projected shell model (PSM). Energy levels of negative and positive parity bands of ^{159}Sm and ^{160}Sm isotopes of Samarium nucleus are obtained separately for each spin. Kinetic and dynamic moments of inertias are also calculated for these isotopes. The acquired results are compared with the experimental data. The electromagnetic reduced transition probabilities, B(M1)/B(E2) the behavior of dynamic moment of inertia J^2, rotational kinetic energy and moment of inertia J^1 as a function of spin have also been investigated and proper comparison is made between the calculated results and the experimental data. The alignment phenomena of neutron-proton pairs in view of the rotational movement in high spin states has also been studied with reference to band crossing.

Keywords: Electromagnetic Reduced Transition Ratio, PSM, Moment of Inertia, Rotational Alignment

1. Introduction

The projected shell model that has been applied in recent years to study the structure of nuclei, especially the nuclei in the lanthanide region, has achieved some success [1]. The most prominent feature of this model is that it exhaustively discusses the spectroscopic data of nuclei with high-spin properties using a basic physical interpretation. Using this model has other advantages such as its simple computational method compared to similar methods and its relatively better results [2, 3]. In 1995, the Nilsson model was developed by Hara and San to describe the deformation characteristics of the axial symmetry of deformed nuclei, and a notion of this new model was recognized as the projected shell model [18]. A couple of years later, a code based on the projected shell model was written for Windows-operated computers, using Fortran programming language. This Fortran code was used to describe the structure of rare-earth heavy nuclei of the periodic table and the results had successfully deduced the experimental data [4]. In mass regain about A~150, deformation in the nuclear shape increases rapidly with a small change in the mass number of isotopes. the level structure of Sm odd-A isotopes was studied by Kenefick and Scheline using this Fortran programming code [5]. Low-lying collective states in odd-even nuclei include one-neutron two-proton quasiparticle and three-quasiparticle configurations with a combination of one neutron plus two protons. In even-even nuclei, these states include zero-quasiparticle vacuum, two-neutron quasiparticle, two-proton quasiparticle, and four -quasiparticle configurations,

involving two neutrons plus two protons [6, 20]. The biggest challenge of this model is related to calculations regarding multi-excited quasiparticle bands for odd-even and even-odd isotopes. Therefore, studying the single particle structure and interactions of nucleons in these isotopes can be considered as a test to assess the validity of this model [7]. As demonstrated in the present study, the projected shell model that describes the yrast lines of the individual odd-even and even-even isotopes of Sm nucleus (150 and 160), efficiently corresponds with the experimental data. Topics discussed in this paper include yrast spectrum changes, structures and configurations of quasiparticle bands, band crossing and variation in moments of inertia, excitation of the neutron $i_{13/2}$ orbital and the proton $h_{11/2}$ orbital as the shell model intruder.

In this study, the calculation results are related to the ground-state band structure of ^{160}Sm isotopes and ^{159}Sm odd-even and even-even isotopes which were carried out using Fortran code based upon the projected shell model. Also, the results are in competent correspondence with the experimental data which clearly indicates the validity of this model. The obtained results of the calculations for quasiparticle alignments in the band crossing are compared with each other by examining the moments of inertia and ratio of electromagnetic reduced transition probabilities for these two isotopes. Yet, none of these studies thoroughly elucidate the structural properties of the whole isotopic chain of odd-mass or even-mass Sm nuclei. The present paper is ordered as follows:

In Section.2, an outline for the PSM formalism is given. It also provides expressions for various physical quantities to be subsequently discussed in this paper. In Section.3, the calculation results are compared with the experimental data. Eventually, the paper is concluded in Secion.4.

2. Brief Overview of the Theory

The projected shell-model PSM is a spherical shell-model that expands on deformed single-particle bases and seems suitable for studying the structure of deformed nuclei [8]. Truncating in this method is done by multi-quasiparticle bases due to selecting intrinsic states. The rotational symmetry for these states is then reconstructed by the projection method from a spherical (multi-particle) base using experimental data. Finally, the resultant Hamiltonian is diagonalized at these bases [9]. single-particle states of the Nilsson model are combined using the results of (Bardeen-Cooper-Schrieffer) BCS calculations and pairing correlations. The outcome of BCS calculations in a set of quasiparticle states is constructed based on a vacuum state (| 0 >) in the intrinsic framework. Please refer to reference [1] for more details on the theory of shell model. The configuration space of the projected shell model for protons and neutrons, generally consists of three major shells. In this paper, the calculations are made considering three major shells (N=4, 5, 6 for neutrons and N=3, 4, 5 for protons), and also by employing deformation parameters of ε_2 (quadrupole) and ε_4 (hexadecapole) for ^{159,160}Sm isotopes [10]. Projection of a set of quasiparticle states ($|\varphi_k>$), consists of zero, two and four quasiparticles for even-even nucleus and states with one, two and three quasiparticles for the odd-even nucleus. For a proper angular momentum, the following configuration spaces are constructed for an even-even and odd-even nucleus, respectively [1, 9]

$$\left\{\left|\Phi_K\right\rangle\right\}=\left\{\left|0\right\rangle.a^+_{\nu1}a^+_{\nu2}\left|0\right\rangle.a^+_{\pi1}a^+_{\pi2}\left|0\right\rangle.a^+_{\nu1}a^+_{\nu2}a^+_{\pi1}a^+_{\pi2}\left|0\right\rangle\right\} \quad (1)$$

$$\left|\Phi_k\right\rangle=a^+_{\nu}\left|0\right\rangle, a^+_{\nu}a^+_{\pi1}a^+_{\pi2}\left|0\right\rangle, \quad (2)$$

with | 0 > as the vacuum state, a $^+$ as the quasiparticle creation operators with index π and ν, (as Nilsson quantum numbers for protons and neutrons) respectively. The momentum projection operator is also described as follows [1]

$$P_{MK}{}^{I}=\frac{2I+1}{8\pi^2}\int d\Omega D_{MK}{}^{I}(\Omega)R(\Omega). \quad (3)$$

Where $\hat{R}(\Omega)$, Ω and D^I_{MK} (Ω) are in order, the rotational operator, the Euler angle and the D-function that forms a complete set of functions in the Ω parameter space by acting on quasiparticle's nucleon-pair states $|\varphi_k>$. The wave functions, $|\Psi_{IM}>$ within the shell model are defined as follows [1]

$$\left|\Psi_{IM}\right\rangle=\sum_K F_K{}^{I}\hat{P}_{MK}{}^{I}\left|\Phi_K\right\rangle. \quad (4)$$

The coefficients F^I_K can be determined using the solutions of the following Schrodinger equation $\hat{H}\left|\Psi_{IM}\right\rangle=E\left|\Psi_{IM}\right\rangle$. This eigenvalue equation can be solved using the Hamiltonian diagonalization based on $\hat{P}_{MK}{}^{I}\left|\Phi_K\right\rangle$, presented as follows [1]

$$\sum_{K'}\left(H_{KK'}{}^{I}-EN^I_{KK'}\right)F^I_{K'}=0. \quad (5)$$

Where the matrix norm elements together with the Hamiltonian are determined as follows [1]

$$N^I_{KK'}=\left\langle\Phi_K\left|\hat{P}^I_{KK'}\right|\Phi_{K'}\right\rangle$$

$$\mathrm{H}^I_{KK'}=\left\langle\Phi_K\left|\hat{\mathrm{H}}\hat{P}^I_{KK'}\right|\Phi_{K'}\right\rangle \quad (6)$$

Eventually, the expectation value of the Nilsson-model Hamiltonian as a function of spin, I, is achieved via the following equation [16]

$$E_K(I)=\frac{\left\langle\Phi_K\left|\hat{\mathrm{H}}\hat{P}^I_{KK}\right|\Phi_K\right\rangle}{\left\langle\Phi_K\left|\hat{P}^I_{KK}\right|\Phi_K\right\rangle}=\frac{\mathrm{H}^I_{KK}}{N^I_{KK}} \quad (7)$$

By including monopole reactions, the total Hamiltonian in the PSM is defined as follows [19, 26]

$$\hat{\mathrm{H}}=\hat{\mathrm{H}}_0-\frac{1}{2}\chi\sum_{\mu}\hat{Q}^+_{\mu}\hat{Q}_{\mu}-G_M\hat{\mathrm{P}}^+\hat{\mathrm{P}}-G_Q\sum_{\mu}\hat{\mathrm{P}}^+_{\mu}\hat{\mathrm{P}}_{\mu}. \quad (8)$$

Here the first term $\hat{H}_0$ is the spherical single-particle Hamiltonian, containing a proper spin-orbit force. In this non-spherical Hamilton, the second, third, and fourth terms are quadrupole-quadrupole, monopole and quadruple-pairing potentials, respectively. The coefficients χ, GM and G_Q represent the strengths of quadrupole-quadrupole, monopole-pairing and quadruple-pairing interactions, respectively. Employing a self-consistent method together with the quadrupole deformation parameter ε_2, the strength χ can therefore be calculated. Also, the monopole-pairing interaction strength G_M, is obtained via the following equation [6, 19]

$$G_M = \left(G_1 \pm G_2 \frac{N-Z}{A} \right) A^{-1} \tag{9}$$

Where (–) and (+) signs correspond to neutrons and protons, respectively. G_1 and G_2 are pairing constants affecting the choice of quasiparticle bases. The quadrupole-pairing interaction strength, GQ is linked to G_M linearly as GQ=ɣ GM. This interaction has a great impact on changing alignment of nucleons outside the nuclear central core. The values of required constants applied in the calculations are shown in table 1 [10, 11].

Table 1. *Deformation parameters, coefficients, G1, G2 and proportional constant ɣ for calculation of two isotopes.*

Isotope	ε_2	ε_4	G_1	G_2	ɣ	Z	N
159	0.27	-0.03	19.6	15.6	0.16	62	97
160	0.27	-0.03	20.12	13.13	0.18	62	98

3. Result and Discussion

As a function of spin, the quasiparticle energies are obtained through the calculations based on the projected shell model. The number of energy bands for ^{159}Sm and ^{160}Sm are 25 and 60, respectively. They can be plotted in a diagram as a group of projection energy levels for different spins in one band for each intrinsic configuration of two isotopes. These diagrams are for unperturbed energy configuration which is obtained before the application of the configuration mixing and are used to interpret the output results of code playing an important role in inferring the numerical results. In addition, band crossing, which is a dominant phenomenon of nucleon pair alignments, is well-defined in such diagrams. Of course, to plot these diagrams, it is not necessary to consider all energy bands, but only those necessary to interpret the results are enough. These diagrams are good tools for testing the capability of quasiparticle configurations used in calculations [1, 9, 21]. The obtained yrast energies are also indicated in these energy diagrams. In Figure 1, the band diagram of the ^{159}Sm isotope is plotted for the grand state band with negative parity. Two one-quasiparticle neutron bands include $1\ \nu_{i\ 13/2}$ [-7/2] k=-7/2 and $1\ \nu_{i\ 13/2}$ [5/2] k=5/2 configurations having the lowest energy state and are close to the yrast line, which are finished at spin 23.5ħ by crossing with two three-quasiparticle bands (formed by one neutron and a pair of protons) with $1\ \nu i_{13/2}$ [-5/2] + $2\pi_{h\ 11/2}$ [1/2, 5/2] k=½ and $1\ \nu_{i\ 13/2}$ [-7/2] + $2\pi h_{\ 11/2}$ [1/2, -5/2] k=-11/2 configurations, forming the yrast band. After spin I=23.5 ħ, these bands dive into the yrast region. The measured values of the yrast band are used from reference [12]. The energy band diagram of ^{160}Sm isotope is indicated in Figure 2. The yrast line is based on a zero-quasiparticle band (g-band) before spin 24 ħ. At spin 24 ħ, two two-quasiparticle neutron bands with $2\nu_{i\ 13/2}$ k=3 [5/2, 1/2] and $2\ \nu_{i\ 13/2}$ k=2[5/2, -1/2] configurations, cross the g-band. Therefore, by decreasing their energy, they approach the yrast line. In Spin 22 ħ, two lowest–lying, two-quasiparticle proton bands consisting of $2\ \pi h_{11/2}$ k=-1 [5/2, -7/2] and $2\pi h_{11/2}$k=-2 [1/2, -5/2] cross the g-band and after decreasing their energy, they do not approach the yrast line. In other word, the rotational energy is unable to align proton pairs. The experimental research data of the yrast band for this isotope is obtained from reference [23].

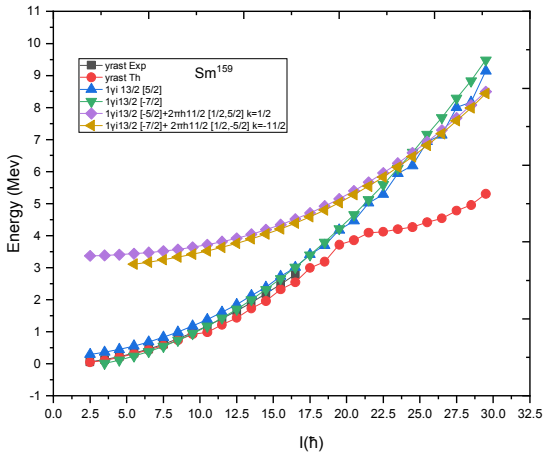

Figure 1. *Band diagram for negative parity bands of ^{159}Sm isotope. Only the important low-lying bands in each configuration are indicated.*

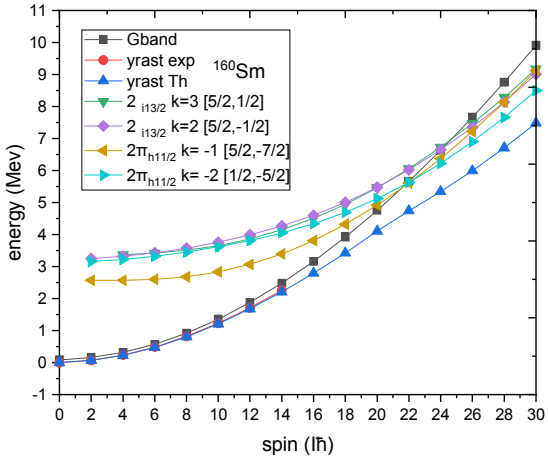

Figure 2. *Band diagram for positive parity bands of ^{160}Sm isotope. Only the important low lying-bands in each configuration is indicated.*

Expected configuration mixing is occurred with 1-quadrupole pairing and 3-quadrupole pairing interactions at proper spin which describes the rotational alignment of $h_{\ 11/2}$-protons in ^{159}Sm and $i_{\ 13/2}$ neutrons in ^{160}Sm isotope. This behavior is well predicted by the results of the present shell model. It is noticed that the rotational frequency $\omega = \left[\frac{E(I) - E(I-2)}{2} \right] \left(\hbar^{-1} Mev \right)$, reach its lowest value in

crossing spin for both isotopes at rotational alignment position [14].

To indicate the variations of the band structure in the crossing spin caused by the rotational alignment, the values of kinetic and dynamic moments of inertia are calculated using the following equations, respectively [13, 14]

$$J^{(1)} = \left[\frac{(2I-1)}{E_\gamma(I)}\right]\left(\hbar^2 Mev^{-1}\right) \quad (10)$$

$$J^{(2)} = \left[\frac{4}{E_\gamma(I+2)-E_\gamma(I)}\right]\left(\hbar^2 Mev^{-1}\right) \quad (11)$$

Figure 3 indicates that, up to spin I=19.5ħ, the amount of J^1 has a constant dip and the theoretical results based on PSM and the experimental data [12] are in good agreement. The values of J^1 increase sharply in spins I=23.5ħ & 24.5ħ. This increase at spin I=23.5 ħ happened due to the crossing of two -one-quasiparticle neutron bands with two- three--quasiparticle proton bands where the most value of J^1 is obtained. The calculated results of J^1 as a function of spin are compared with the experimental data which are shown in Figure 4. As it is clear from this figure, the calculated values of J^1 for ^{160}Sm are varied slowly up to spin 20ħ. Finally, at spin 24ħ, it shows an extended increase due to the crossing of g-band with two two-quadrupole pairing neutron bands. The comparison of kinetic moment of inertia diagrams for two isotopes, indicated that the variation of this quantity as a function of spin for these isotopes is not alike due to their different nuclear structure and sudden increment of this quantity for ^{159}Sm than the ^{160}Sm isotope. It can be seen from Figure 5 that calculated variations of dynamic moment of inertia as a function of spin with at I=3.5 ħ, have more fluctuations than for I=4.5 ħ. Subsequently, the J^2 value increases in the spin region I=4.5 ħ to I=17.5 ħ with a smooth dip and then decreases in spin I=21.5 ħ. Finally, it increases in band crossing spin. The calculated results are in good correspondence with the experimental gamma energy data [12] up to spin I=15.5 ħ.

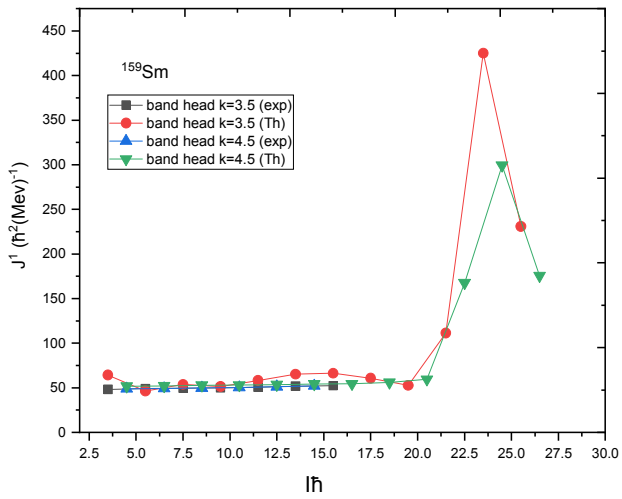

Figure 3. *The calculated moment of inertia, J^1 as a function of spin for ^{159}Sm isotope are compared with experimental data [12].*

Figure 6 shows the values for dynamic moment of inertia as a function of spin for ^{160}Sm isotope. As can be seen from this figure, J^2 is an ascending function of the spin up to the spin I=24 ħ. In the spin range I=14 ħ to I=24 ħ with an almost constant dip, it reaches a maximum value at spin I=24 ħ. Then it decreases with increment of spin. In fact, the constant dynamic moment of inertia indicates that the transition energy division for different spins is almost constant. However, the dynamic moment of inertia is a very sensitive quantity as it describes the variation of J^1. It is also a good tool for indicating changes in band structure at band crossing spin [24, 25].

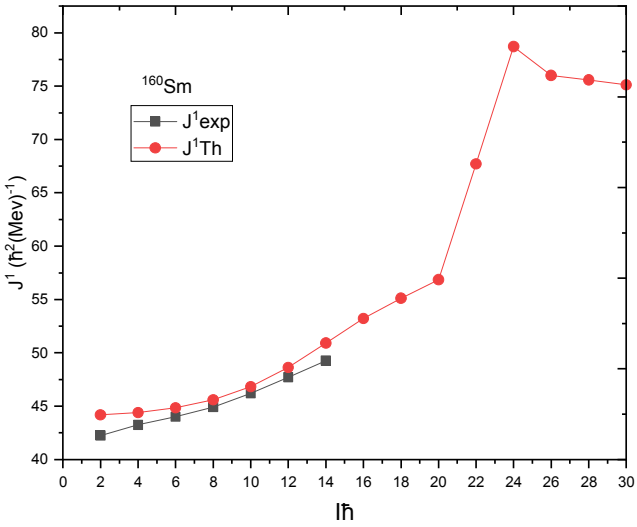

Figure 4. *The calculated moment of inertia, J^1 as a function of spin for ^{160}Sm isotope is compared with the experimental data [2].*

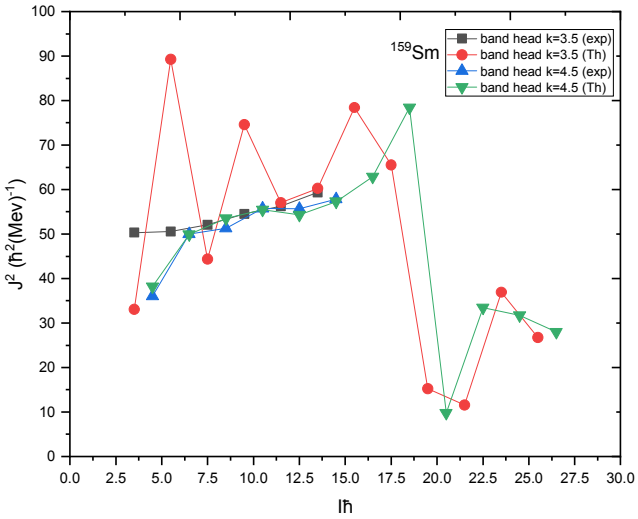

Figure 5. *The comparison of experimental [12] and calculated data J^2 (dynamic moment of inertia) as a function of spin for ^{159}Sm.*

Dipole (ΔI=1) transition energies of the ground state for negative-parity bands of ^{159}Sm isotope is shown in Figure 7. As it is clear from this figure, the calculated values using the PSM are in good correspondence with the experimental data up to spin I=12.5 ħ. The predicted values of the PSM are in the form of zigzags and as can be seen from Figure 7, the variation of transition energy, changes after the band crossing spin (I=23.5 ħ). This indicates that the spin alignment of the

one-neutron quasiparticle blokes the two-proton quasiparticle alignment. In addition, the diagram for the variation of energy transition as a zigzag pattern, shows the effects of energy level splitting [14, 24].

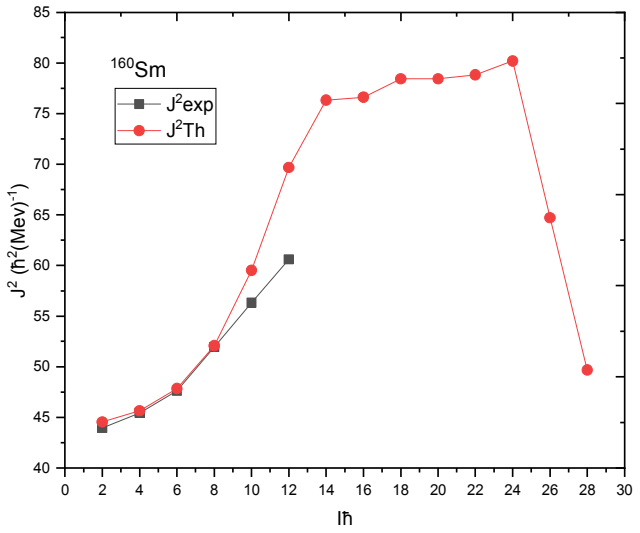

Figure 6. *Comparison of experimental data [23] and calculated results of J^2 (dynamic moment of inertia) as a function of spin for ^{160}Sm.*

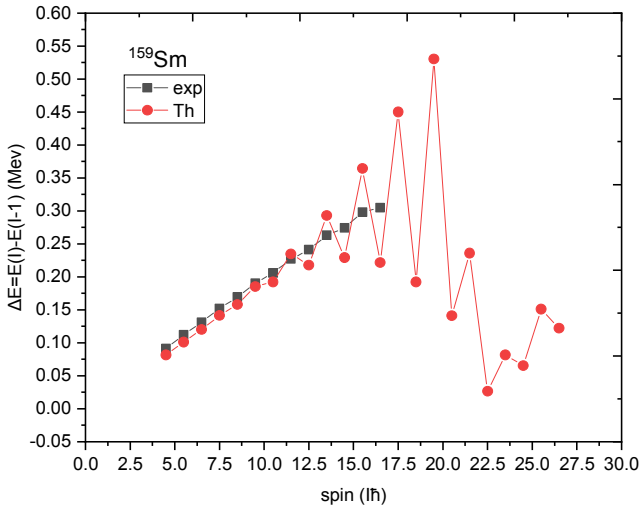

Figure 7. *Comparison of theoretical and experimental transition energy E(I)-E(I-1) versus the angular momentum I for ^{159}Sm.*

The reduced electromagnetic transition ratio probability B (M1)/B (E2), provides useful data on the structure of rotational bands. The calculated results of reduced transition probability are used to obtain the electric quadrupole and magnetic dipole moment of isotopes [15]. The following equations are employed to calculate the electric quadrupole, magnetic dipole and their ratio for ^{159}Sm and ^{160}Sm isotopes, respectively,

$$B(E2) = \frac{816}{E_\gamma^5 \tau_P} e^2 fm^4 Mev^5 ps \tag{12}$$

$$B(M1) = \frac{56.8}{E_\gamma^3 \tau_P} \mu_N^2 Mev^3 ns \tag{13}$$

$$\frac{B(M1)}{B(E2)} = 0.69 E_\gamma^2 \frac{\mu_N^2}{e^2 b^2} \frac{1}{Mev^2}. \tag{14}$$

The calculated results of the reduced electromagnetic transition ratio probability are indicated as a function of spin for ^{159}Sm and ^{160}Sm isotopes in Figures 8 and 9, respectively. This quantity strongly depends on the pairing of the orbitals and therefore the comparison between theoretical and experimental data helps to identify the quasiparticle configuration [16, 17]. The reduced electromagnetic transition ratio of the ground state for the ^{159}Sm isotope as a function of spin is compared with the experimental research data [12] which is obtained from the measured gamma-ray energies for spins $3.5\hbar$ and $4.5\hbar$ head bands separately as in Figure 8. In spin $3.5\hbar$, the value of this ratio is very small and its value increases as the spin rises up to 19.5.

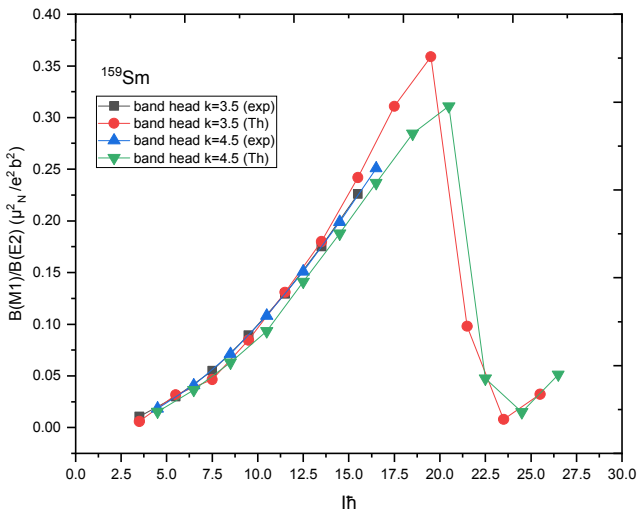

Figure 8. *Comparison of experimental data with the calculated ratio of reduced electromagnetic transition probabilities B(M1)/B(E2) as a function of spin [12] for ^{159}Sm.*

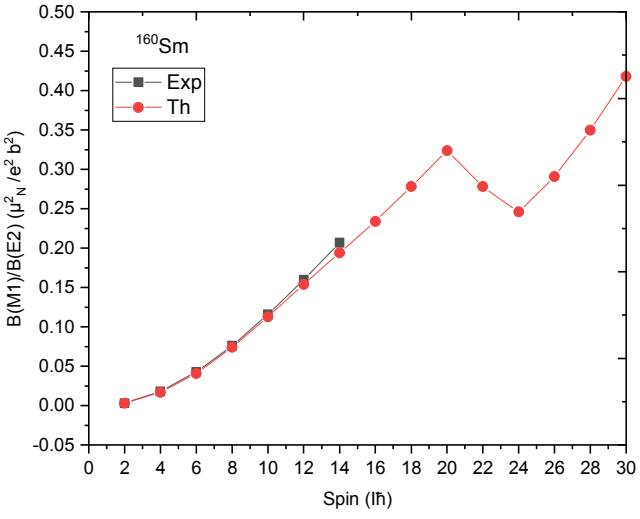

Figure 9. *Comparison of experimental data with the calculated ratio of reduced electromagnetic transition probabilities B(M1)/B(E2) as a function of spin [23] for ^{160}Sm.*

In the case when the main behavior of the isotope is initially

an electrical quadrupole structure, with an increase in angular momentum, the rotational motion of the isotope is changed, therefore it leads to an increase in the contribution of magnetic dipole structure. Finally, in the band crossing spin (I=23.5 $\hbar$), due to the alignment of proton pairs in the π $h_{11/2}$ state, the rotational motion of the isotope decreases suddenly after increasing the moment of inertia, thus the isotope reaches its initial state with the least rotation and leads to reduction in the dipole magnetic manner of isotope.

The Calculated and experimental B(M1)/B(E2) ratios for ^{160}Sm isotope are compared in Figure 9 and presented in table 2. The ratios is increased up to spin I=20$\hbar$. The predicted values of B(M1)/B(E2) show a reduction at spin I=24$\hbar$, it then increases up to spin I=30 $\hbar$. In other words, as nuclear rotational motion increases due to the alignment of $i_{13/2}$ two-quadrupole pairing interaction of neutrons at I=24 $\hbar$, the rotating motion suddenly decreases with an increase in moment of inertia, and this is associated with a reduction in the dipole magnetic properties. The most dipole magnetic properties, as a result of PSM, occur in spin I=30$\hbar$. There is a good agreement between experimental data and calculated results based on PSM up to spin I=14$\hbar$.

Calculated kinetic moment of inertia J^1, dynamic moment of inertia J^2 and reduced electromagnetic transition probability of ^{160}Sm and ^{159}Sm are compared with experimental data in tables 2 and 3, respectively.

Table 2. *Calculated values of moments of inertia (J^1 & J^2) and BM1/BE2 of ^{160}Sm.*

Spin	J^1 (exp) ħ2 $(MeV)^{-1}$	J^1 (Th) ħ2 $(MeV)^{-1}$	J^2 (exp) ħ2 $(MeV)^{-1}$	J^2 (Th) ħ2 $(MeV)^{-1}$	BM1/BE2 TH μ2N/e2 b2	BM1/BE2exp μ2N/e2 b2
2	42.253	44.184	43.95	44.54	0.0031	0.0031
4	43.253	44.388	45.45	45.66	0.0171	0.018
6	44	44.843	47.61	47.84	0.041	0.043
8	44.91	45.606	51.94	52.083	0.074	0.076
10	46.22	46.832	56.33	59.52	0.113	0.116
12	47.71	48.635	60.6	69.68	0.154	0.16
14	49.27	50.915		76.33	0.194	0.207
16		53.2193		76.62	0.234	0.0672
18		55.121		78.43	0.278	
20		56.865		78.43	0.324	
22		67.71		78.83	0.278	
24		78.71		80.2	0.246	
26		76		64.72	0.291	
28		75.58		49.68	0.35	
30		75.12			0.418	

4. Conclusion

The following results are achieved through the calculated results based on the PSM and their comparison with the experimental data for ^{159}Sm and ^{160}Sm isotopes:

The kinetic and dynamic moments of inertia, ratios B(M1)/B(E2) and the transition energy from the excited bands to the ground state band are calculated for ^{159}Sm to indicate the alignment effect of nucleon pairs on the band crossing spin of ^{159}Sm and ^{160}Sm isotopes. Moreover, the variation of these values as a function of spin are presented in Figures 1 to 9. These figures clearly indicate that for both isotopes, the calculated results of band crossing and the alignment of nucleon pairs in the upper spin region are well predicted by PSM, which is explained by the fact that the level density becomes higher in this region of the spin. This may occur for well-deformed isotopes. Moreover, the levels become closer to each other resulting in band crossing and alignment of nucleon pairs. However, for some isotopes, this may happen in the lower spin area. Also, for well-deformed isotopes, it will occur in the upper spin region [2, 22]. In general, the change in the calculated values in the band crossing spin region for two isotopes of Samarium (159 and 160) shows that the diagrams of calculated values related to the ^{159}Sm isotope are smaller than those related to the ^{160}Sm isotope caused by differences in the band structure due to the presence of an unpair nucleon in the ^{159}Sm isotope. The expected blocking of three-quadrupole pairing alignment of single-neutron with a slight increase in J^2 in to spin I=20.5 $\hbar$ followed by a change in its behavior after spin I=23.5 $\hbar$ as well as the behavior of the zigzag energy transition can be accounted to the coupling of bands 1 $\nu i_{13/2}$ [-7/2] k=-7/2 and 1 $\nu i_{13/2}$ [5/2] for the ^{159}Sm isotope. In general, for both isotopes the band structure changes after band crossing spin.

Table 3. *Calculated values of moments of inertia(J^1 & J^2) and BM1/BE2 and transition energy E(I)-E(I-1) of ^{159}sm isotope for band head spin I=3.5.*

Spin	J^1 (exp) ħ2 $(MeV)^{-1}$	J^1 (Th) ħ2 $(MeV)^{-1}$	J^2 (exp) ħ2 $(MeV)^{-1}$	J^2 (Th) ħ2 $(MeV)^{-1}$	E (I)-E (I-1) exp MeV	E (I)-E (I-1) Th MeV	BM1/BE2 TH μ2N/e2 b2	BM1/BE2exp μ2N/e2 b2
3.5	48.27	64.37	50.31	33.05	0.0719		0.0059	0.0106
5.5	49.06	46.51	50.56	89.28	0.1123	0.101	0.0318	0.03
7.5	49.48	53.88	52.08	44.34	0.1518	0.1415	0.0465	0.055
9.5	50.041	51.42	54.5	74.62	0.1902	0.1853	0.0845	0.0892
11.5	50.8	58.3	56.25	57.02	0.227	0.2347	0.131	0.1294
13.5	51.751	65.31	59.34	60.23	0.2631	0.2931	0.1801	0.1754
15.5	52.41	66.25		78.43	0.2982	0.3643	0.242	0.226
17.5		60.74		65.54		0.4501	0.311	

Spin	J^1 (exp) ħ2 $(MeV)^{-1}$	J^1 (Th) ħ2 $(MeV)^{-1}$	J^2 (exp) ħ2 $(MeV)^{-1}$	J^2 (Th) ħ2 $(MeV)^{-1}$	E (I)-E (I-1) exp MeV	E (I)-E (I-1) Th MeV	BM1/BE2 TH μ2N/e2 b2	BM1/BE2exp μ2N/e2 b2
19.5		52.63		15.23		0.5305	0.359	
21.5		111.43		11.56		0.2358	0.098	
23.5		425.13		36.93		0.0817	0.008	
25.5		230.94		26.73		0.1511	0.0323	

Table 4. *Calculated values of moments of inertia(J1&J2) and BM1/BE2 and transition energy E(I)-E(I-1) of ^{159}sm isotope for band head spin I=4.5.*

Spin	J^1 (exp) ħ2 $(MeV)^{-1}$	J^1 (Th) ħ2 $(MeV)^{-1}$	J^2 (exp) ħ2 $(MeV)^{-1}$	J^2 (Th) ħ2 $(MeV)^{-1}$	E(I)-E(I-1) exp MeV	E (I)-E (I-1) Th MeV	BM1/BE2 TH μ2N/e2 b2	BM1/BE2exp μ2N/e2 b2
4.5	48.96	51.865	36.03	38.16	0.0915	0.0816	0.0154	0.0184
6.5	49.342	52.17	50	49.93	0.1311	0.1201	0.0364	0.04087
8.5	49.8	52.98	51.28	53.5	0.1695	0.1581	0.0629	0.0712
10.5	50.466	53.03	55.78	55.5	0.2061	0.1922	0.09328	0.1083
12.5	51.271	53.6	55.71	54.3	0.2411	0.2178	0.1412	0.1511
14.5	52.112	54.34	57.803	57.3	0.2742	0.2292	0.1879	0.1989
16.5		54.61		62.89	0.3049	0.2216	0.2368	0.2509
18.5		56.04		78.43		0.1922	0.2846	
20.5		59.55		9.77		0.1411	0.311	
22.5		167.74		33.41		0.0265	0.0474	
24.5		299.315		31.74		0.0654	0.0149	
26.5		175.63		27.97		0.1222	0.05136	

References

[1] K. Hara and Y. Sun, Projected shell model and high-spin spectroscopy, *Int. J. Mod. Phys. E* 4, 637 (1995). https://doi.org/10.1142/S0218301395000250.

[2] K. Hara and Y. Sun Studies of high-spin states in rare-earth nuclei using the angular momentum projection method, *Nucl. Phys.* A529, 445 (1991). https://doi.org/10.1016/0375-9474(91)90580-Y.

[3] R. Devi, B. D. Sehgal, and S. K. Khosa and J. A. Sheikh, Projected shell model description of high spin states in ^{124}Ce, *Phys. Rev.* C 72, 064304 (2005). https://doi.org/10.1103/PhysRevC.72.064304.

[4] M. Shahriarie, S. Mohammadi and Z. Firouzi, study of back bending in ^{157,158}Er isotopes by using electromagnetic reduced transition probabilities, *J. Korean Phys. Soc. 76, 8 (2020).* https://doi.org/10.3938/jkps.75.1.

[5] R. A. Kenefick, R. K. Sheline Level Structure of the Odd-A Isotopes of Samarium, *phys. Rev*. 139, 1479 (1965). https://doi.org/10.1103/PhysRev.139.B1479.

[6] J. A. Sheikh, G. H. Bhat, Y. Sun, G. B. Vakil, and R. Palit, Triaxial projected shell model study of γ-vibrational bands in even-even Er isotopes, *Phys. Rev.* C 77, 034313 (2008). https://doi.org/10.1103/PhysRevC.77.034313

[7] Y.-X. Liu, Y. Sun, X.-Zhou, Y.-Zhang, S.-Y. Yu, Y.- C. Yang and H. Jin, A systematical study of neutron-rich Zr isotopes by the projected shell model*, Nucl. Phys*. A 858, 11 (2011). https://doi.org/10.1016/j.nuclphysa.2011.03.010.

[8] K. Hara, Y. Sun, Studies of high-spin states in rare-earth nuclei using the angular-momentum projection method, Signature splitting in odd mass nuclei, *Nucl. Phys. A* 537, 77 (1992) https://doi.org/10.1016/0375-9474(92)90157-F.

[9] Y. Sun and K. Hara, Fortran code of the Projected Shell Model *Comput*. *Phys*. *Commun*. 104, 245 (1997). https://doi.org/10.1016/S0010-4655(97)00064-7.

[10] P. Muller, A. J. Sierk, T. Ichikawa and H. Sagawa, Nuclear ground-state masses and deformations, At*. Data Nucl. Data Tables* 109, 1 (2015). https://doi.org/10.1016/j.adt.2015.10.002.

[11] R. K. Pandit, S. Sharma, R. Devi, S. K. Khosa, microscopic study of band structures of neutron rich ^{153,155,157}sm isotopes. *Eur. Phys. J. Plus*. 135, 830 (2020). https://doi.org/10.1140/epjp/s13360-020-00845-3.

[12] Christopher Jason Zachary, New Insights Into the Structure of Neutron Rich Nuclei ^{157}Sm, ^{163}Gd, and ^{163}Tb, Ph.D. thesis of Graduate School of Vanderbilt University, Vanderbilt University. Pro Quest Dissertations Publishing, 2019. 13811714.

[13] S. J. Asztalos, I. Y. Lee, K. Vetter, B. Cederwall, Spin yields of neutron-rich nuclei from deep inelastic reactions, *Phys. Rev. C* 60, 044306 (1999), https://doi.org/10.1103/PhysRevC.60.044306.

[14] L. M. Chen, R. S. Guo, The Projected Shell Model Description of the Yrast Bands in Super deformed Thallium Nuclei, *Chinese Journal of Physics*. 47, 788 (2009).

[15] M. Mahmoud, signature splitting and signature inversion of rotational bands in odd-odd nuclei in rare-earth region, Turk J Phys, 33 (2009) 333-350 https://doi.org/10.3906/fiz-0904.

[16] B. Alex Brown, Lecture Notes in Nuclear Structure Physics (National Superconducting Cyclotron Laboratory and Department of Physics and Astronomy, Michigan State University, E. Lansing, MI 48824, (2005).

[17] P. Verma, C. Sharma, S. Singh, A. Bharti, S. K. Khosa, G. H. Bhat, J. A. Sheikh, projected shell model study of quasiparticle structure of arsenic isotopes. 918, 1 (2013). https://dx.doi.org/10.1016/j.nuclphysa.2013.09.005.

[18] R. K. Pandit, R. K. Bhat, R. Devi and S. K. Khosa, G. H. Bhat and J. A. Sheikh, microscopic study of electromagnetic properties and band spectra of neutron deficient ^{133,135,137}Sm*. Chinese Physics C* 43, 12 (2019). https://doi.org/10.1088/1674-1137/43/12/124108.

[19] S. G. Nilsson, Binding states of individual nucleons in strongly deformed nuclei, *Dan. Mat. Fys. Medd. 29 (16) 1 (1955).*

[20] R. Devi, B. D. Sehgal and S. K. Khosa Projected shell model study of neutron deficient ^{122}Ce, *pramana Journal of Physics* 67 (3), 467 (2006), https://DOI:10.1007/s12043-006-0007-z.

[21] K. Hara and S. Iwasaki, On the quantum number projection: (I). *General theory Nucl. Phys*. A 332, 61 (1979). https://doi.org/10.1016/0375-9474(79)90094-0.

[22] Y. Sun and J. L. Egido, Angular-momentum-projected description of the yrast line of dysprosium isotopes, *Nucl. Phys. A* 580, 1 (1994), https://doi.org/10.1016/0375-9474(94)90811-7.

[23] S. Iwasaki and K. Hara, Treatment of the Band Crossing by Means of the Angular Momentum Projection Method, *Prog. Theo. Phys*. 68, 1782 (1982). https://doi.org/10.1143/PTP.68.1782.

[24] H. Mach, A. Piotrowski, R. L. Gill, R. F. Casten, and D. D. Warner, Identification of Four New Neutron-Rich Rare-Earth Isotopes, *Phys. Rev. Lett*. 56, 1547 (1986). https://doi.org/10.1103/PhysRevLett.56.1547.

[25] A. Iba´nez-Sandoval and M. E. Ortiz, V. Velazquez, A. Galindo-Uribarri, P. O. Hess, Y. Sun, Projected shell model study of yrast states of neutron-deficient odd-mass Pr nuclei, *Phys. Rev. C* 83, 034308 (2011). https://doi:10.1103/physRevC.83.03408.

[26] Y. Sun, L. J. Wang, F.-Qi Chen, T. Mizusaki, M. Oi, and P. Ring, Recent developments of the projected shell model Based on many-body techniques, EPJ Web of Conferences 93, 01017 (2015). https://doi:10.1051/epiconf/20159301017.